

Quasiresonant Vibration \leftrightarrow Rotation Transfer in Atom-Diatom Collisions

Brian Stewart, Peter D. Magill, Thomas P. Scott,^(a) Jacques Derouard,^(b) and David E. Pritchard

*Chemistry and Physics Departments and Research Laboratory of Electronics,
Massachusetts Institute of Technology, Cambridge, Massachusetts 02139*

(Received 28 September 1987)

We have performed an extensive level-resolved experimental study of vibrotationally inelastic collisions in this system $\text{Li}_2^*(v_i, j_i) + \text{Ne} \rightarrow \text{Li}_2^*(v_f = v_i + \Delta v, j_f = j_i + \Delta j) + \text{Ne}$, with $8 \leq j_i \leq 76$. At high j_i , the rate of vibrational transfer is large, exceeding the purely rotationally inelastic rate, and extremely specific, populating only a few rotational levels per Δv . The most probable Δj obeys the rule $\Delta j = -4\Delta v$. These effects are enhanced at low collision velocity and are quite insensitive to v_i and the target gas. Classical trajectory calculations reproduce these results.

PACS numbers: 34.50.Ez, 34.50.Pi

We present a level-resolved study of vibrotationally inelastic (VRI) atom-diatom collisions, which demonstrates that a new type of vibrational transfer occurs at large rotational quantum numbers. At high j_i the total rate constant for vibrational inelasticity in the Li_2^* -Ne system is very large, corresponding to a cross section of over 100 \AA^2 and substantially exceeding the purely rotationally inelastic (RI) rate constant. In addition, the cross section for vibrotational transfer increases with decreasing velocity at large j_i , just the opposite of what occurs at the low j_i that have been studied in most experiments¹ and calculations.^{2,3} Under these conditions, Δv and Δj become highly correlated, leading to very specific final rotational distributions. These observations, suggested by previous trajectory calculations⁴⁻⁶ and our preliminary experiments,⁷ are fully elaborated in the experimental work presented here, which is compared with successful attempts to model this behavior with use of classical trajectories.⁸ We call the phenomena quasiresonant vibration \leftrightarrow rotation (V \leftrightarrow R) transfer to emphasize the narrow j_f distribution observed while stressing that changes in the vibrational and rotational quantum numbers (not energies) are the correlated variables.

The experimental apparatus and data analysis are essentially the same as in our work on rotationally inelastic collisions.⁹ A temperature-stabilized stainless steel oven contains lithium metal and neon gas at 600°C . Lithium molecules (present at about 0.1 Torr in the vapor) are excited to a single ($A^1\Sigma_u^+$) rovibronic level by a single-mode cw dye laser. Fluorescence from the excited Li_2 molecules is collected and dispersed; the resulting spectrum contains lines emanating from the laser-populated level (parent lines) and from levels populated by inelastic collisions (satellite lines). This spectrum is measured at four or five neon pressures between 0.2 and 3.0 Torr. The lines are assigned, and ratios of satellite to parent intensity are determined after correction for line strength and instrument response. Fits to the pressure dependence of these ratios determine the rate constants. Measurement of the fluorescence spectrum for a number

of vibrational bands enables us to make several determinations of each rate constant in most cases, permitting us to identify transitions polluted by spectral interference and increasing our confidence in the measured rates.

Because the laser is tuned to line center for our rate-constant measurements, only molecules with no velocity component along the laser axis are excited; the distribution of collision velocities is therefore not a Maxwell-Boltzmann distribution at the temperature of the cell. However, it has been demonstrated⁹ that the actual distribution of collision velocities is very well approximated by a Maxwell-Boltzmann distribution at a lower temperature T_{eff} . Our data contain three pairs of forward-backward rate constants that satisfy detailed balance within error at T_{eff} , enhancing our confidence in our experimental procedures. T_{eff} is about 700 K for all the data in this study, corresponding to a mean thermal velocity of $1.35 \times 10^5 \text{ cm s}^{-1}$.

We also present velocity-dependent cross sections that were obtained by the method of velocity selection by Doppler shift (VSDS).¹⁰ This technique entails our tuning the laser over the Doppler profile (thus varying the range of selected Li_2 speeds) while simultaneously monitoring the parent fluorescence and fluorescence from a satellite line of interest. The dependence of the rate constant on the relative velocity of the collision partners is then deconvolved from the resulting line shapes with use of mathematical and data-processing procedures developed previously.^{10,11} Normalizing these velocity-dependent rate constants to the measured thermally averaged rate constants gives the velocity dependence of the rate constants, and hence the cross section, to an accuracy of about 15%.

Results of quasiclassical trajectory calculations are included for comparison with the data. The trajectories were calculated by an action-angle technique¹² that incorporates the vibrational coupling. The interaction potential is based on one that was used to model RI results¹³; it is an exponentially repulsive breathing ellipsoid. No attempt was made to optimize the potential for

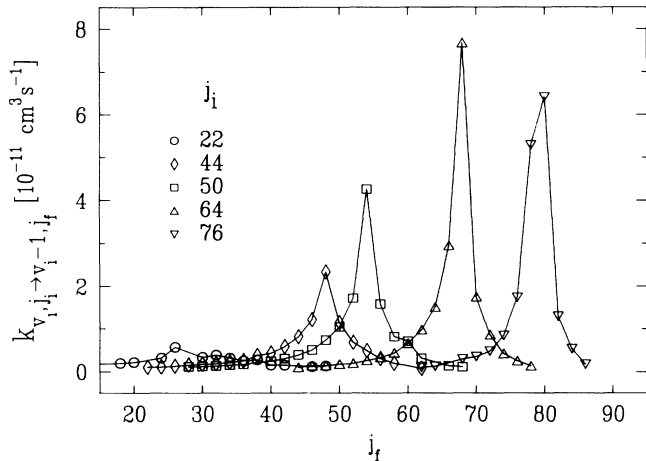


FIG. 1. The rapid rise of the VRI rate constant and narrowing of the j_f distribution with increasing j_i are shown by our experimental data for $\Delta v = -1$. The distribution of j_f is narrowest for $j_i = 64$, only $3h$ FWHM. The droppoff of the $j_i = 76$ rate is due in part to the increase of rate constants for $|\Delta v| > 1$. Experimental uncertainties are about the size of the symbols.

this VRI work; the qualitative agreement obtained is quite insensitive to the potential parameters, in accord with experimental results on target gases ranging from Ne to Xe.¹⁴ Cross sections were calculated by the standard histogram method, and thermally averaged rate constants were obtained from a six-point Gauss-Laguerre integration of the cross sections.

We now turn to the major results of the study:

(1) *The VRI rate constant rises dramatically as j_i increases, and becomes increasingly sharply peaked at a specific j_f .* Figure 1 shows the experimental data for $\Delta v = -1$ and j_i ranging from 22 to 76. The peaking of the rate constant with j_f is strongest at $j_i = 64$, with a value of over $8 \times 10^{-11} \text{ cm}^3 \text{ s}^{-1}$, corresponding to a level-to-level cross section of about 8 \AA^2 . The j_f distribution has a full width at half maximum of only 3 at this j_i . Although experimental exigencies precluded the maintenance of a constant v_i throughout the study, comparison of previous data¹⁴ at $v_i = 9$, $j_i = 42$ with the present $v_i = 4$, $j_i = 44$ data shows that the dependence of the rates on v_i is weaker than the linear dependence predicted by the Landau-Teller theory. The startling j_i dependence is far and away the dominant effect in the data presented here.

(2) *Δv and Δj are highly correlated at the peak of the j_f distributions.* Figure 2(a) shows the systematic shift in j_f^{peak} with Δv for $-3 \leq \Delta v \leq 2$ at $j_i = 64$. Here the rule $\Delta j^{\text{peak}} = -4\Delta v$ holds, as it does for $j_i = 44$ and 50 as well. This is not the same as the criterion for intramolecular energy resonance, $\Delta j^{\text{peak}}/\Delta v = -\omega_e/2B_e j_i$, which is 4 for $j_i = 64$, but 6 for $j_i = 44$; for this reason, we term the process *quasiresonant*. The classical trajec-

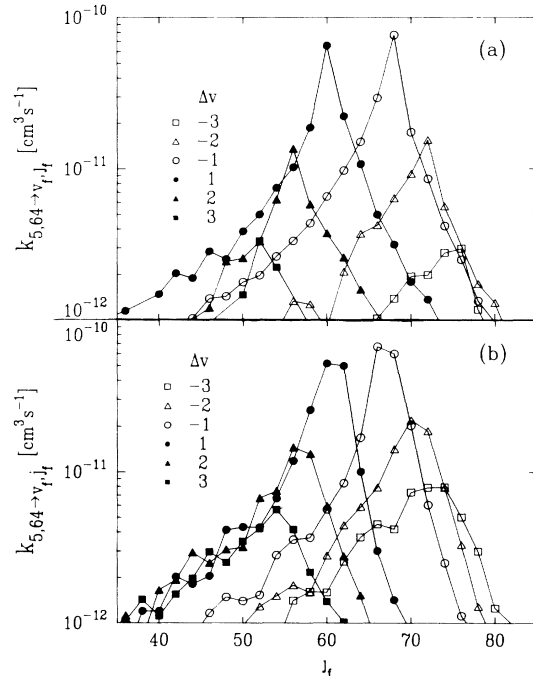


FIG. 2. (a) Experimental rate constants for $-3 \leq \Delta v \leq 3$, with $j_i = 64$, show the systematic shift of Δj with Δv , given by the rule $\Delta j^{\text{peak}} = -4\Delta v$. (b) Results of thermally averaged classical trajectory calculations mimic the behavior of the data, although the breadth of the j_f distributions is larger than in the experimental rate constants (see text).

tories of Fig. 2(b) capture the observed j_f dependence well, although the distributions are somewhat broader than the experimental ones because the quasiclassical bins are nearly as broad as the sharp j_f distributions themselves.

(3) *The quasiresonant peaking of the rate constant is enhanced at low collision velocity.* Figure 3(a) displays velocity-dependent cross sections obtained in a VSDS study¹⁵ of Li_2^*-Ne at $v_i = 9$, $j_i = 42$. It is apparent that the j_f distribution is very sharply peaked at low velocity, with a full width at half maximum of only 3 at the lowest studied velocity of $6 \times 10^4 \text{ cm/s}$, and a peak value of 3.5 \AA^2 . Figure 3(b) demonstrates that this phenomenon is qualitatively reproduced by the quasiclassical trajectories, although the overall scale and range of velocities differ from the experimental data.

(4) *The quasiresonant process is quite insensitive to the nature of the interaction potential.* Data taken at $j_i = 42$ with target gases ranging from He to Xe show¹⁴ that the $\Delta v = -1$ rates for Ne through Xe are the same to within a scale factor, even though Li_2^*-Xe is substantially more attractive than Li_2^*-Ne .¹³ In addition, the variation of the parameters in the potential used in our trajectory calculations, or even the substitution of an altogether different potential, made little difference in the outcome at large j_i . Moreover, quasiresonant peaking

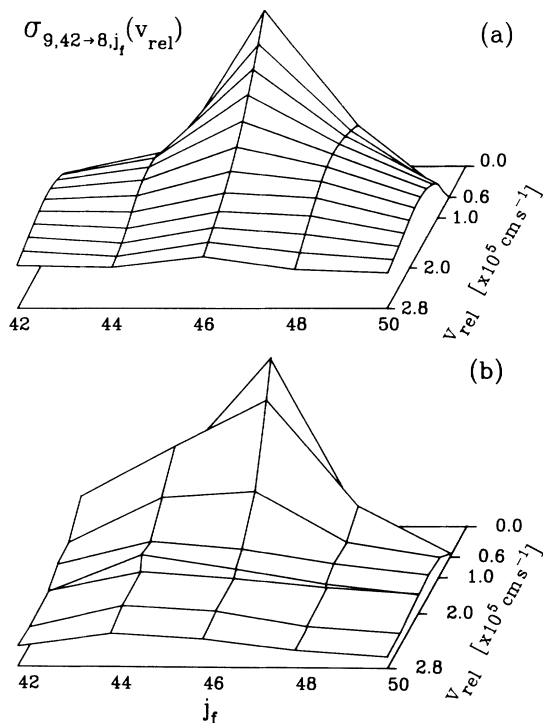


FIG. 3. (a) The velocity-resolved experimental cross section for $\Delta v = -1$ and $j_i = 42$ rises as velocity decreases and becomes strongly peaked at the quasisonant value $j_f = 46$. The peak value of the cross section is 3.4 \AA^2 . The absolute error in the experimental cross sections is about 15%. (b) Quasiclassical trajectories reproduce the velocity dependence of the data, although the overall scales differ; the peak cross section is 8.7 \AA^2 . Relative errors in the calculated cross sections are about 10%.

has been observed in trajectory calculations on $\text{H}_2\text{-He}^{4-6}$ and HCl-Ar^{16} with totally dissimilar potentials.

(5) *VRI collisions dominate RI collisions at large j_i .* Experimental rate constants summed over final rotational levels are displayed in Fig. 4. The total inelastic rate constant declines slightly as j_i increases from 8 to 76 because of the plummeting RI rate, which offsets the rapidly increasing VRI rate. At $j_i = 64$, collisions that change v are the dominant inelastic process, and by $j_i = 76$, the rate constants for $|\Delta v| > 1$ constitute almost half the total VRI rate constant. In this regime, theories that neglect rotation, decouple it from the vibration, or treat it as a perturbation (i.e., the majority of current models) are obviously unable to treat the VRI processes observed here.

We believe that the enhancement of the vibrationally inelastic rate results from an increase in the effective speed at which the atom encounters the end of the molecule as a result of the rapid molecular rotation. As pointed out by Blais and Truhlar,⁴ the rotationally enhanced collision speed augments the component of the time-dependent force at the oscillator frequency, increasing the probability of vibrational transfer. Scrutiny of

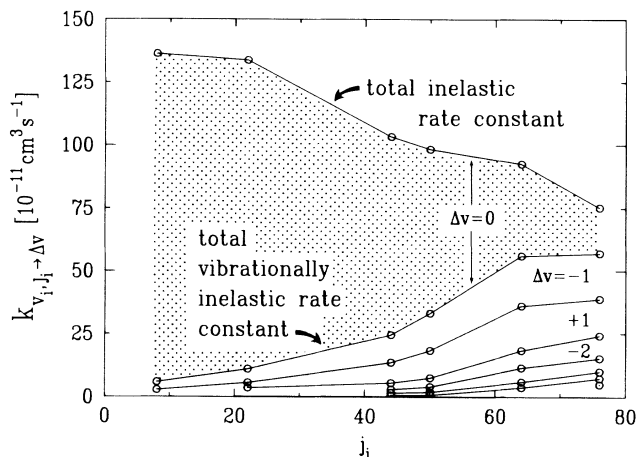


FIG. 4. Rotationally summed rate constants for each of the Δv measured. The top line is the total inelastic rate constant, the next line is the total vibrationally inelastic rate constant. The separation of these lines is the total rotationally inelastic rate constant, and the separations of successive lines are the rate constants for $\Delta v = -1, +1, -2, +2$, etc. The rotationally inelastic rate constant (shaded) falls dramatically as j_i increases, becoming a small fraction of the total inelastic rate constant at high j_i .

the time evolution of individual classical trajectories has confirmed this observation and revealed additional information about the collision dynamics.⁸ These observations, and the experimentally observed enhancement of the effect at low velocity, imply that the details of the interaction are dominated by the rotation rather than the translation.¹⁷ Further support for this explanation is provided by measurements on $\text{I}_2^* - \text{X}$ ($\text{X} = \text{He}, \text{Xe}$),¹⁸ which show none of the features of quasisonance even at $j_i = 91$. With a moment of inertia over an order of magnitude greater than Li_2 , I_2 cannot achieve rotational speeds great enough to modulate the atom-molecule force significantly at the vibrational frequency at experimentally accessible j_i values.

In summary, we have documented a new type of $\text{V} \leftrightarrow \text{R}$ transfer that occurs because of high initial rotation and results in very specific final level distributions. Apart from its intrinsic scientific interest, this process is obviously relevant in the relaxation of any gas containing light, rotationally hot molecules. In addition, it may serve as a mechanism for the production of rotationally excited molecules from a vibrationally excited sample; molecules that acquire rotational excitation during the initial stage of relaxation may cascade to yet higher rotational levels via quasisonant $\text{V} \leftrightarrow \text{R}$ transfer, possibly producing a rotational inversion in the ground vibrational level. This mechanism could be important in the relaxation of H_2 formed in a laboratory trap or interstellar cloud, and may provide the inversion mechanism in hydrogen halide rotational lasers.

We are grateful to Richard Stoner for his assistance in

obtaining and analyzing the data. This work was supported by National Science Foundation Grant No. CHE-8421392.

^(a)Present address: VenturCom Inc., 215 First St., Cambridge, MA 02142.

^(b)Permanent address: Laboratoire de Spectrométrie Physique, Université Scientifique et Médicale de Grenoble, B.P. 87, 38402 Saint-Martin-d'Hères Cédex, France.

¹G. Hall, K. Liu, M. J. McAuliffe, C. F. Giese, and W. R. Gentry, *J. Chem. Phys.* **78**, 5260 (1983).

²H. R. Mayne, *J. Chem. Phys.* **81**, 2684 (1984).

³D. R. Flower and D. J. Kirkpatrick, *J. Phys. B* **15**, 1701 (1982).

⁴N. C. Blais and D. G. Truhlar, *J. Chem. Phys.* **69**, 846 (1978), and *J. Phys. Chem.* **86**, 638 (1982).

⁵J. E. Dove, S. Raynor, and H. Teitelbaum, *Chem. Phys.* **50**, 175 (1980).

⁶D. L. Thompson, *J. Chem. Phys.* **75**, 1829 (1981).

⁷K. L. Saenger, N. Smith, S. L. Dexheimer, C. Engelke, and

D. E. Pritchard, *J. Chem. Phys.* **79**, 4076 (1983).

⁸P. Magill, B. Stewart, N. Smith, and D. E. Pritchard, to be published.

⁹T. P. Scott, N. Smith, and D. E. Pritchard, *J. Chem. Phys.* **80**, 4841 (1984).

¹⁰N. Smith, T. P. Scott, and D. E. Pritchard, *J. Chem. Phys.* **81**, 1229 (1984).

¹¹N. Smith, T. A. Brunner, and D. E. Pritchard, *J. Chem. Phys.* **74**, 467 (1981).

¹²N. Smith, *J. Chem. Phys.* **85**, 1987 (1986).

¹³N. Smith, Ph.D. thesis, Massachusetts Institute of Technology, 1982 (unpublished).

¹⁴P. Magill, T. Scott, B. Stewart, N. Smith, and D. E. Pritchard, to be published.

¹⁵T. Scott, B. Stewart, N. Smith, P. Magill, and D. E. Pritchard, to be published.

¹⁶D. L. Thompson, *J. Phys. Chem.* **86**, 630 (1982).

¹⁷Using the rotational frequency for $j_i = 64$ (1.0×10^{13} rad/s) and an interaction length of $3-4 \text{ \AA}^2$, we obtain an effective collision velocity several times the thermal velocity at the temperature of the experiment.

¹⁸S. L. Dexheimer, T. A. Brunner, and D. E. Pritchard, *J. Chem. Phys.* **79**, 5206 (1983).

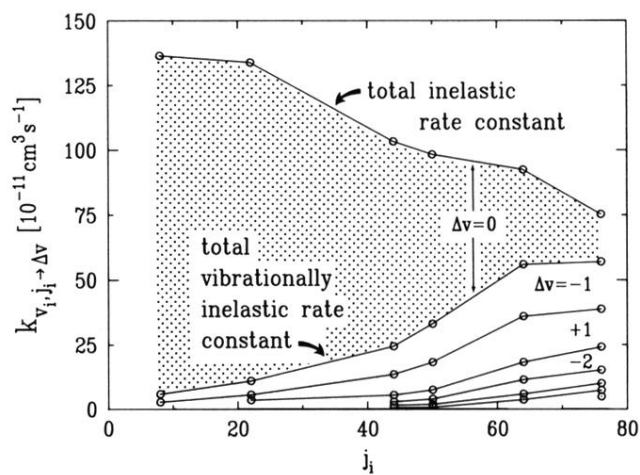


FIG. 4. Rotationally summed rate constants for each of the Δv measured. The top line is the total inelastic rate constant, the next line is the total vibrationally inelastic rate constant. The separation of these lines is the total rotationally inelastic rate constant, and the separations of successive lines are the rate constants for $\Delta v = -1, +1, -2, +2$, etc. The rotationally inelastic rate constant (shaded) falls dramatically as j_i increases, becoming a small fraction of the total inelastic rate constant at high j_i .